

Anti-corrosion Process of *Epiphyllum oxypetalum* Extract on Aluminum Alloy in Acidic Environment

Francis Okechukwu Nwosu^{1*}

¹Department of Physics/Electronics, Abia State Polytechnic, Aba, Nigeria.

Author's contribution

The sole author designed, analysed, interpreted and prepared the manuscript.

Article Information

Editor(s):

(1) Dr. Yang Qu, Heilongjiang University, China.

Reviewers:

(1) Nkem B. Iroha, Federal University Otuoke, Nigeria.

(2) Abubakar Shehu Mohammed, Abubakar Tafawa Balewa University, Nigeria.

(3) Olatunde Alaba Akinbulumo, Obafemi Awolowo University, Nigeria.

Complete Peer review History: <http://www.sdiarticle4.com/review-history/57465>

Original Research Article

Received 23 March 2020

Accepted 29 May 2020

Published 30 May 2020

ABSTRACT

Major problems encountered in industries, science and engineering is corrosion failure. The gravimetric, the electrochemical impedance spectroscopy (EIS) technique and Vickers hardness test were employed in investigating the anti-corrosion process of Aluminum alloy in acidic environment (0.5 M HCl solution) using *Epiphyllum oxypetalum* leaf extract. The leaf extraction was prepared using reflux set-up. Addition of the leaf extract in the corrosive media significantly reduced the mass loss and the corrosion (damage) rate. The inhibition efficiency increased linearly with the inhibitor concentration with a peak value of 89% for gravimetric technique and 87% for EIS technique, but slightly reduced with temperature rise. The charge-transfer resistance, R_{ct} increased linearly with the increase in concentration of the inhibitor in the corrosive environment. The Vickers's microindentation hardness test investigated revealed a preservation of the indentation value of the AA5052 exposed to inhibitive environment compared with those exposed to uninhibited environment. Surface screening was conducted and examined the surface morphology of the metals before, and after exposure to the various inhibitive solution. The experimental data obeyed Langmuir adsorption isotherm. Thermodynamic parameters (heat of adsorption, ΔH^{\ddagger} , activation energy, E_a , entropy, ΔS^{\ddagger} and Gibb's free energy, ΔG_{ads}) were evaluated through the Eying and Arrhenius plots. Upon the addition of the inhibitor, ΔH and E_a increased while the ΔS^{\ddagger} decreased.

Keywords: Corrosion; adsorption; AA5052; gravimetric; electrochemical; *Epiphyllum oxypetalum*.

*Corresponding author: Email: nwosufranciso@yahoo.com;

1. INTRODUCTION

A report by Karthik and Sundaravadivelu [1] has it that the environmental consequence of corrosion is enormous and its inhibition has been deeply investigated by researchers. Organic compounds recently have captured researcher's attention especially in the area of corrosion inhibition. The inhibition ability of an organic molecules depends on their efficiencies to adsorb on the surface of the metals. Inhibitive impacts of organic molecules are usually based on the substitution of H₂O molecules from the metal surface and formation of barrier film of the inhibitor compound on the surface of the metal [2,3]. The use of corrosion inhibitors is one of the most practical and economical methods for diminishing corrosion rates and the protection of metal surfaces against corrosion [4].

Adsorption of inhibitors on ingot surface is a function of some inhibitor group physicochemical properties not limited to the following: density of the electron at the donor atom, the nature and surface charge of the metal, the type of aggressive electrolyte, orbital character and electronic structure of the molecule (the chemical structure of the inhibitors) [5,6]. The process of inhibitor's action is critically on the surface of the adsorbent. Further, efficiency of a given inhibitor depends on the characteristics of the environment in which it acts, the nature of the metal surface and electrochemical potential at the interface [7].

The position of aluminum and its alloy in the industries, and homes are very enormous to mention. Aluminum is known as the third abundant element on the earth crust [8]. The corrosion resistance ability and the mechanical properties of Al-alloy are in constant attack as a result of service condition, environmental treat, and other factors. Due to their wide usage, there is need to seek for a way of maintaining and protecting the metal against environmental attack especially as acid is mostly applied in the cleaning and pickling process. Acid have been found as a cleaning agent of aluminum alloys. Thus, the use of *Epiphyllum oxypetalum* leaf extract drew attention on the need to the combat to corrosion attacks of Aluminum alloy, AA5052 in acidic environment.

2. MATERIALS AND METHODS

2.1 Materials Preparation

The metal, AA5052 alloy were mechanically cut into coupons of sizes, 20 mm x 20 mm x 1.5 mm

for the gravimetric studies, while a size of 1 mm x 1 mm x 1 mm was sectioned for electrochemical studies. The metal was prepared according to ASTM G1 (2003) [9] early employed by [9,10]. The coupons were weighed using electronic weighing balance of 0.0001 sensitivity.

The leaf extraction was conducted using Reflux setup. The leaf harvested within Abia State Polytechnic, Aba (5.1338°N, 7.3554°E) were ground to powder called stock. The stock extracted into the corrosive environment in the ratio 1:30. The solute-solvent mixture was subjected to heating at a temperature (60°C). And the various concentrations of the inhibitor were prepared from the filtrate using (C₁V₁ = C₂V₂). The solvent used for the extract is 0.5 M HCl.

2.2 Gravimetric Technique

The gravimetric technique involves taking note of the initial weight of the metal immersed in the corrosive environment and the final weight after the corrosion inhibition process. The final weight of the coupons was measured after the corrosion and the inhibition process. The procedure outlined on ASTM G31-72(2004) [10] STANDARDS were followed for reliability. The system of immersion practice was planned interval test. The corrosion inhibition process involved full immersion of the coupon in 0.5 M HCl solution containing the various concentrations of the inhibitor without disturbance was. The setup was allowed for a maximum period of 9-hours under ambient temperature and each coupon retrieved every 1-hour corrosion process quenched. The temperature of the environments was raised to 45°C and 60°C using water-bath for 2-hours. The process was carried out three times for reproducibility and the average value reported.

2.3 Electrochemical Impedance Spectroscopy (EIS) Technique

Electrochemical methods are used in many different ways to assess the effectiveness of corrosion inhibitors and coatings for metals and alloys [11]. Electrochemical impedance spectroscopy (EIS) has been an advanced technique used in corrosion investigations. The EIS studies the system response to the application of a periodic small amplitude ac signal [12]. Electrochemical Workstation Potentiostat/Galvanostat electrochemical analyzer with a tripod stand: The working

electrode being the coupon (AA5052), the reference electrode and the counter electrode were used. Before measurement, the working electrode was immersed in test solution (0.5 M HCl containing different concentrations of the leaf inhibitor) for approximately 30-minutes until a steady open-circuit potential (OCP) was reached. The EIS was performed at -0.25 to +0.40 volts versus open circuit potential, at a scan rate of ± 0.333 volts per second, step height of 1.0 mm and a step time of 3 seconds. The data obtained from the electrochemical tests were analyzed using Echem analyst 5.0 software. To confirm the reliability and reproducibility of the electrochemical issues, duplicate experiments organized for each case, and under the same conditions. And the average value was reported. The following electrochemical parameters were determined: solution resistance, R_s , charge transfer resistance, R_{ct} , corrosion rate and the inhibition efficiency (from the equation 3).

2.4 Micro indentation Hardness Test

Microindentation hardness test (MHT) was used due to the size of the metal coupon. Three sets of aluminum alloy ingot were used in carrying out the mechanical hardness test. The AA5052 alloy was exposed to 0.5 M HCl corrosive solution containing *Epiphyllum oxypetalum* leaf extract at the various concentrations. The test was conducted according to ASTM Designation E 384 – 99 [13]. The Vickers indenter was notched at a face angle of $136^\circ \pm 30''$ with a test force (HV 10) of 10 kgf for 10 s randomly (four different locations) across the surface of the metal. The mean hardness value (HV) was reported.

3. RESULTS AND DISCUSSION

3.1 Weight Loss and Corrosion Rate

Weight loss being a measurable change in corrosion process was employed in the study. Fig. 1 depicts the mass loss of Aluminum Alloy, AA5052 in 0.5 M HCl solution. The mass loss of the AA5052 alloy immersed in corrosive environment (blank) increases with exposure time except at the third hour of exposure where the non-ferric metal exhibited passivation phenomenon. Significantly, the presence of the *Epiphyllum oxypetalum* extract in 0.5 M HCl solution hinders the material's mass loss. This hinderance increases with increase in concentrations of the inhibitor.

The time dependent of the material deterioration was calculated using equation 1 [14]. Fig. 2 reported the corrosion rate against the exposure period. The plot exposed that the corrosion rate greatly reduced when the green leaf extract (in different concentrations) were added in the corrosion environment. The trend of the curves suggests that the attack on the metal in the corrosive environment followed the same mechanism of corrosion response. This corrosion rates decreases with an increase in the exposure period in the inhibition systems; and with the inhibitor concentration.

$$CR = \frac{K\Delta W}{At\rho} \quad (1)$$

Where CR is the corrosion rate, K is corrosion constant (which dependent on the parametric measurement of the Area), t is the exposed period (hours), ρ is the density of the metal (gram/dm^3), and ΔW is the weight loss (gram).

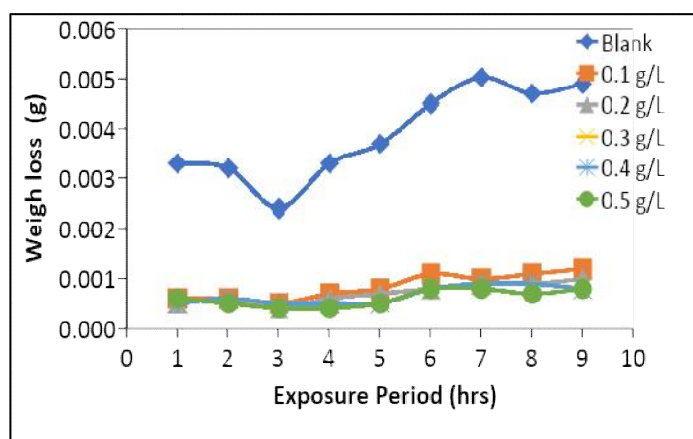


Fig. 1. Weight loss against exposure period of AA5052 in 0.5 M HCl in the presence of *Epiphyllum oxypetalum* extract

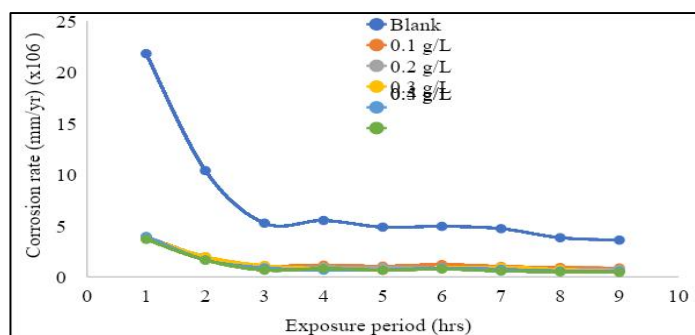


Fig. 2. Corrosion rate against exposure period of AA5052 in 0.5 M HCl in the presence of *Epiphyllum oxypetalum* extract

3.2 Electrochemical Impedance Spectroscopy (EIS) Results

The EIS is an advanced technique greatly enables the investigation of electrochemical processes occurring at the metal/solution interface. The impedance response of the AA5052 alloy in 0.5 M HCl solution containing the various concentration of *E. oxypetalum* extract are presented in the Nyquist plot (Fig. 3). The Nyquist Encirclement diameter increases with increase in the green extract concentration in then corrosive solution inferring that the corrosion process is controlled by charge transfer reaction [15]. The EIS data were fitted adequately by a circuit model shown in Fig. 4. The electrochemical parameters reported on table 1 showed that the value of charge transfer resistance and the solution resistance generally increases linearly with increasing inhibitor concentration. The higher the R_{ct} values, the slower the corrosion process. The formed inhibitive film hinders the diffusion of aggressive ions to the aluminum alloy surface; thus, caused an increase in R_{ct} values in presence of inhibitor [16]. The Nyquist plot from the circuit model developed a capacitive loop following the inductive loop. The complex Nyquist plot has two half-planes: the half-plane capacitive loop and half-plane inductive loop. The increase in the capacitive and inductive loops with the increased concentration of *E. oxypetalum* suggests that the impedance of the inhibited substrate increases.

3.3 Corrosion Inhibition Efficiency

The green leaf inhibition's abilities were considered using the two explored techniques: Gravimetric and Electrochemical Impedance Spectroscopy. The gravimetric focused on the material weight loss (equation 2) [17] while the EIS considers the charge-transfer resistance

(equation 3) [16]. The inhibition efficiency was deployed to determine the impact of the green leaf extract on AA5052 corrosion attack.

$$\%IE = \left(\frac{W_a - W_b}{W_a} \right) \times 100 \quad (2)$$

$$\eta_{EIS}\% = \left(\frac{R_{ct} - R'_{ct}}{R_{ct}} \right) \times 100 \quad (3)$$

Where W_a and W_b are the weight loss of the uninhibited coupon and the inhibited coupon, respectively. R_{ct} and R'_{ct} are the charge-transfer resistance of the corrosion-free environment and the inhibited environment, respectively. The charge transfer resistance was calculated based on the difference between impedance values at the lower and higher frequencies. $\%IE$ and η_{EIS} are the inhibition efficiency for the gravimetric technique and the EIS, respectively.

Considering the gravimetric studies, the inhibition efficiency of *Epiphyllum oxypetalum* extract on aluminum alloy AA5052 (shown in Fig. 5) generally increases with increasing inhibitor concentration with an optimal value of 88% for fourth-hour exposed period. Similar trend was observed for the EIS technique (Table 2). Both techniques showed that the inhibition efficiency of *E. oxypetalum* leaf extract functions as a good corrosion inhibitor for AA5052. The somewhat sinusoidal wave form of the inhibition efficiency curve experienced (in Fig. 5) with the gravimetric technique is possibly attributed to the inherent passivity phenomenon associated with parent metal of the alloy [18].

3.4 Temperature Effect

Variation in temperature of the environments was conducted to determine the influence it would have on the inhibition ability of *E. oxypetalum*

leaf extract. Table 2 shows that the inhibition efficiency of *E. oxypetalum* extract on AA5052 alloy and; it decreased slightly with increase in temperature for every inhibitor concentration. The inverse relationship suggested that the adsorbed molecules of the inhibitor dissolve with increasing temperature. The temperature

increase tends to increase the average kinetic energy of the adsorbed molecules. This causes an increase in the solubility. However, the inhibitor, *E. oxypetalum* showed high inhibition efficiency suggesting its availability even at high temperature range in the fight against corrosion of metals.

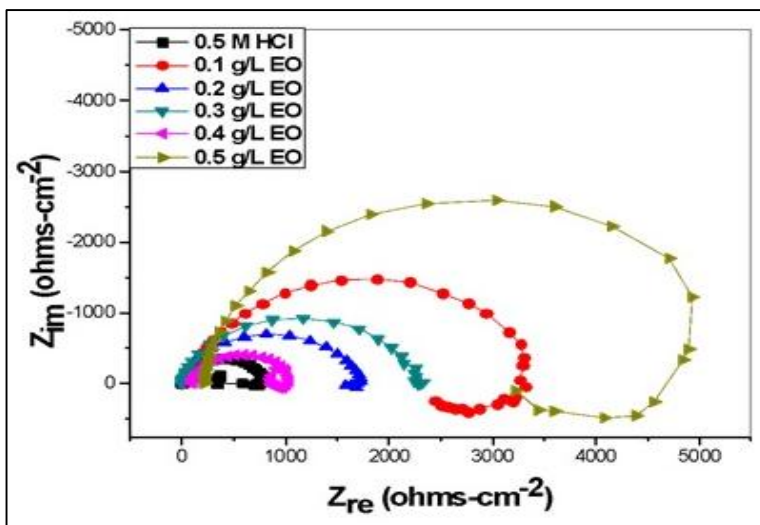


Fig. 3. Electrochemical impedance spectroscopy plots of AA5052 in 0.5 M HCl solution in the absence and presence of different concentrations of *E. oxypetalum*

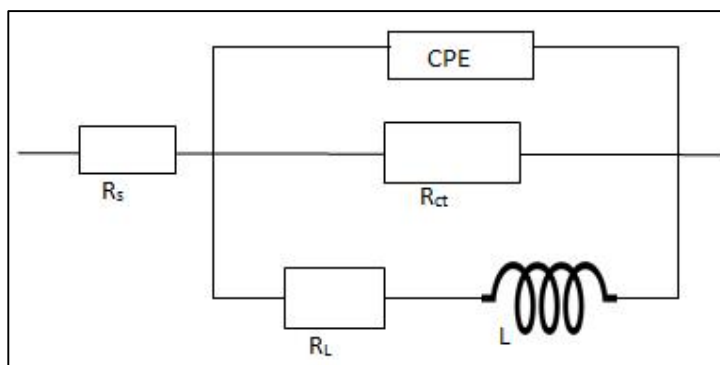


Fig. 4. Equivalent circuit used in fitting the electrochemical impedance spectra

Table 1. Electrochemical parameters of the aluminum alloy, AA5052 in the active environment of 0.5 M HCl solution containing of *E. oxypetalum*

| Environment <i>E. oxypetalum</i> (g/L) | R_s (Ωcm^2) | R_{L1} (Ωcm^2) | R_{ct} (Ωcm^2) | L (H) |
|--|-------------------------------|----------------------------------|----------------------------------|-------|
| 0.0 | 3.03 | 7.8 | 607 | 5.6 |
| 0.1 | 3.55 | 642 | 1128 | 651 |
| 0.2 | 3.93 | 3202 | 1857 | 1607 |
| 0.3 | 3.99 | 2007 | 2489 | 2112 |
| 0.4 | 4.13 | 2543 | 3345 | 2789 |
| 0.5 | 4.26 | 2983 | 4685 | 3365 |

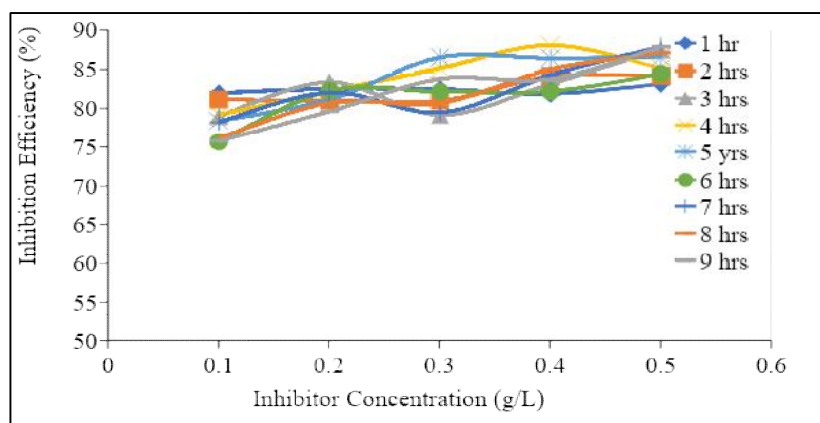


Fig. 5. Inhibition efficiency of *E. oxypetalum* on AA5052 alloy immersed in 0.5 M HCl solution

Table 2. Inhibition efficiency of *E. oxypetalum* leaf extract on AA5052 immersed in 0.5 M HCl solution

| CONC. (g/L) | EIS | | | |
|-------------|-------|-------|-------|-------|
| | 303 K | | 318 K | |
| 0.1 | 46.2 | 81.18 | 75.75 | 74.34 |
| 0.2 | 67.3 | 81.06 | 76.02 | 75.12 |
| 0.3 | 75.6 | 81.03 | 76.92 | 74.78 |
| 0.4 | 81.8 | 84.14 | 79.08 | 76.15 |
| 0.5 | 87.1 | 84.20 | 80.57 | 78.87 |

3.5 Adsorption Models and Thermodynamic Parameters

Adsorption exists due to the presence of the inhibitor molecules and the metal surface. The interaction which arises due to this phenomenon forms the basis for investigating the difference adsorption modes [19]. Langmuir adsorption and the Temkin Adsorption models were exposed to the experimental data and were fitted by the Langmuir adsorption isotherm. Langmuir isotherm model expresses the relationship between the surface coverage and the inhibitor concentration. The Langmuir expressed in equation 4 [20,21] showed that the experimental data were in agreement with the isotherm model plotted in Fig. 6. The plot shows that the Langmuir parameter for the varied temperature conditions all exhibited linear relationship with a slope and correlation coefficient, R^2 approximated to unity (shown in Table 3). The recorded parameter shows that adsorption of the leaf extract follows the Langmuir adsorption isotherm.

$$\frac{C_{inh}}{\theta} = \frac{1}{K_{ads}} + C_{inh} \quad (4)$$

Where θ is the surface coverage, C_{inh} is the inhibitor concentration, and K_{ads} is the adsorption equilibrium constant. The standard free energy of adsorption, ΔG_{ads}° can be calculated from the adsorption equilibrium constant, K_{ads} shown in equation 5.

$$\Delta G_{ads} = -2.303RT \log(55.5K_{ads}) \quad (5)$$

Where R is the gas constant ($8.314 \text{ J mol}^{-1} \text{ K}^{-1}$), and T is the absolute temperature (K). The negative values the standard Gibb's free energy of adsorption with the range below -40 KJ mol^{-1} estimated that the molecules of the *E. oxypetalum* were physically adsorbed on the metal surface at all temperature exposures. This is in line with the general concept highlighted by [22,23], that the values of ΔG_{ads}° around -20 KJ mol^{-1} are consistent with the electrostatic interaction between the charged metal (physical adsorption); whereas those more than -40 KJ mol^{-1} involves charge sharing or transfer from the inhibitor molecules to the metal surface leading to the formation of a donor-acceptor bond (chemical adsorption). Also, the negative value of ΔG_{ads}° indicates spontaneity in the inhibitor adsorption on aluminum alloy, AA5052 surface.

The heat of adsorption, the adsorption energy and activation energy has been reported by [24] as the most important inter-related and frequently calculated parameters relevant to the thermodynamics of any sorption system. Thermodynamically, the activation energy of the corrosion process was calculated from the Arrhenius equation (equation 6) [21,25], which was then rearranged to equation 7 for clarity. The Eyring transition state equation (equation 8) [26] was employed to determine the enthalpy of adsorption (being the heat released or adsorbed during the adsorption process), and the entropy of adsorption using the gravimetric measurements. The equation 8 was linearized to equation 9. The Arrhenius temperature-dependent plot (Fig. 7) and the Eyring transition state plot (Fig. 8) gave straight lines with coefficient regression close to unity.

$$CR = Ae^{-\frac{E_a}{RT}} \tag{6}$$

$$\text{Log}CR = \frac{-E_a}{2.303RT} + \text{Log}A \tag{7}$$

$$CR = \left(\frac{RT}{N_a h}\right) \exp\left(\frac{\Delta S^*}{R}\right) \exp\left(\frac{-\Delta H^*}{RT}\right) \tag{8}$$

$$\text{Log}\left(\frac{CR}{T}\right) = \frac{-\Delta H^*}{2.303R} \left(\frac{1}{T}\right) + \left[\text{Log}\frac{R}{N_a h} + \frac{\Delta S}{2.303R}\right] \tag{9}$$

Where A is the pre-exponential factor, R is the universal gas constant 8.3145 J/mol, T is the absolute temperature (K), N_a is the Avogadro's number $6.022 \times 10^{23} \text{ mol}^{-1}$, h is the Plank's constant $6.626 \times 10^{-34} \text{ J.s}$, E_a is the activation energy, ΔS^* is the entropy of adsorption and ΔH^* is the enthalpy of adsorption.

Table 4 presents the calculated thermodynamic parameter from the Arrhenius and Eyring plots. The E_a of the inhibited systems were greater than that of the inhibited-free system. This establishes that the presence of the inhibitor increased the threshold energy for the corrosion process to take place; conventionally it increased the energy barrier for the corrosion process. Also, the ΔH^* increase on the addition of the inhibitor supports the concept of physical adsorption of the inhibitor substance on the metal surface [27]. The E_a values shows strong inhibitive. The less negative entropy of adsorption in the inhibited system compared with the inhibitor-free environment elaborates on the ordered arrangement of the *E. oxypetalum* molecules on the AA5052 surface. This confirms the surface coverage close to unity and it further bare forth the understanding that complex inhibitor molecules associate rather than dissociates on the metal surface [28-30].

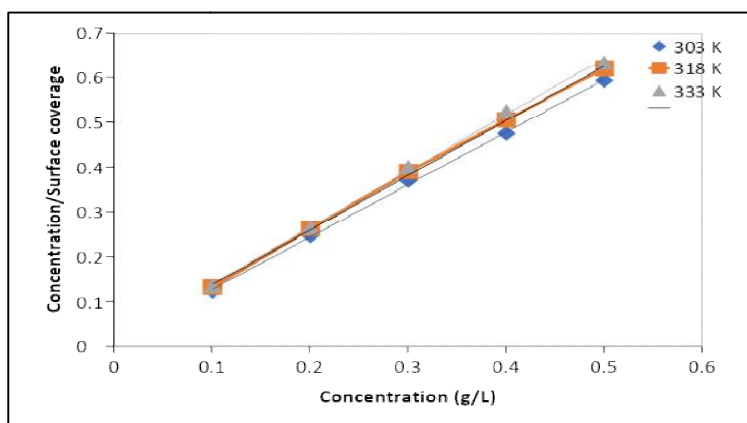


Fig. 6. Langmuir isotherm plot of corrosion of AA5052 in 0.5 M HCl containing *Epiphyllum oxypetalum* leaves extract

Table 3. Langmuir adsorption parameters of *E. oxypetalum* extract in 0.5 M HCl solution

| Temp. (K) | Langmuir Isotherm | | | |
|-----------|-------------------|----------------|------------------|----------------------------|
| | Slope | R ² | K _{ads} | ΔG _{ads} (KJ/mol) |
| 303 | 1.1697 | 0.9999 | 91.7431 | -21.5057 |
| 318 | 1.2200 | 0.9990 | 61.3497 | -20.4918 |
| 333 | 1.2580 | 0.9980 | 67.1141 | -20.7181 |

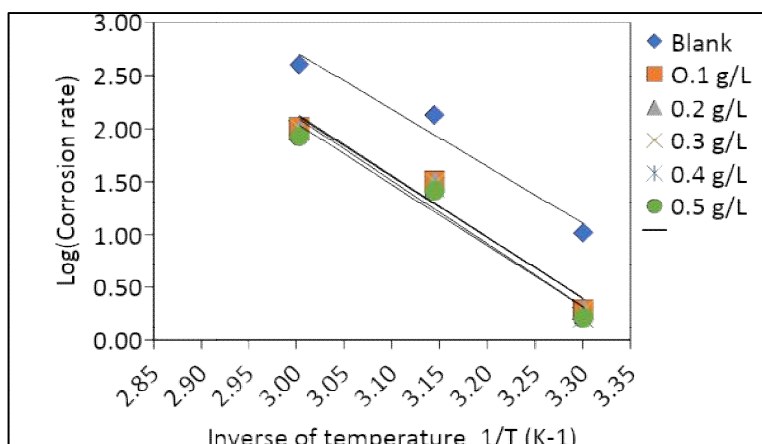


Fig. 7. Arrhenius plots of corrosion of AA5052 alloy in the presence and absence of *E. oxypetalum* extract in 0.5 M HCl

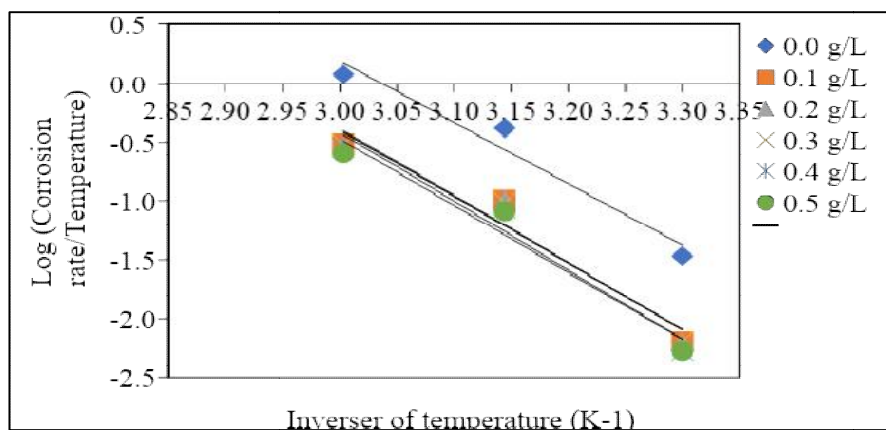


Fig. 8. Eyring plots of corrosion of AA5052 the absence and presence of *E. oxypetalum* extract in 0.5 M HCl solution

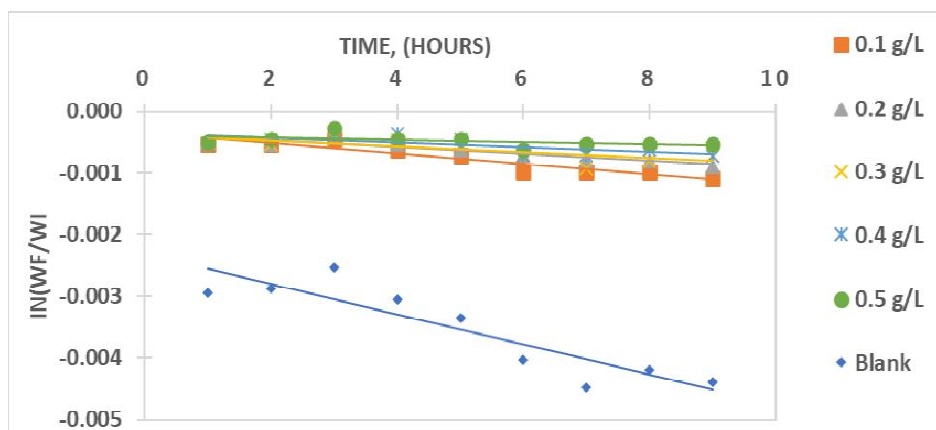


Fig. 9. Plot of $\ln(W_f/W_i)$ against time for AA5052 alloy immersed in 0.5 M HCl solution containing different concentration of *E. oxypetalum* extract

Table 4. Thermodynamics parameters for AA5052 alloy corrosion in 0.5 M HCl solution containing *Epiphyllum oxypetalum* leaves extract

| System <i>E. oxypetalum</i> (g/L) | Activation energy, E_{ads} (KJ/mol) | $A \times 10^{19}$ (L/mol-s) | Enthalpy, ΔH (KJmol ⁻¹ K ⁻¹) | Entropy, ΔS (Jmol ⁻¹ K ⁻¹) | Rate constant k | Half-life |
|--------------------------------------|--|---------------------------------|--|--|------------------------|-----------|
| 0.00 | 102.793 | 0.67 | 43.49 | -65.46 | -2.57×10^{-4} | 2828.43 |
| 0.10 | 111.546 | 4.2 | 47.29 | -58.85 | -8.27×10^{-5} | 8379.67 |
| 0.20 | 110.499 | 2.8 | 46.83 | -60.32 | -5.60×10^{-5} | 12386.94 |
| 0.30 | 110.810 | 3.1 | 46.97 | -59.92 | -4.71×10^{-5} | 14718.54 |
| 0.40 | 114.268 | 10.0 | 48.47 | -55.60 | -3.92×10^{-5} | 17682.26 |
| 0.50 | 111.014 | 2.79 | 47.06 | -60.29 | -1.87×10^{-5} | 37096.74 |

First order reaction kinetics with respect to AA5052 in 0.5 M HCl solution were observed when $\ln(W_f/W_i)$ was plotted against time according to the equation 10. The plot (Fig. 9) was used to obtain the rate constant and subsequently the half-life of the ingot in the environment using equation 11.

$$\ln \frac{W_f}{W_i} = -kt \tag{10}$$

$$t_{1/2} = \frac{0.693}{k} \tag{11}$$

Where W_f is the final weight after immersion, W_i is the weight before immersion, K is the rate constant and t is time. $t_{1/2}$ is the half-life of the aluminum alloy.

The obtained rate constant has inverse relationship with time; but a direct relationship with the inhibitor concentration. However, the calculated half-life shows a very significant increase when the inhibitor concentrations were added. Conversely, the presence of the inhibitor

greatly influenced the half-life of the AA5052 in 0.5 M HCl environment.

3.6 Surface Morphology Examination

Surface screening examination was executed on three categories of the aluminum alloy, AA5052 after 9 hours of exposure shown in Fig. 10. sample (a) is the raw coupon (as bought), showing how the nature of the surface is before any corrosion and corrosion inhibition process. Sample (b) is coupon exposed to corrosive media without inhibitor. The surface is characterized by roughness linked to the attack of the aggressive media resulting to metal dissolution. However, the addition of *E. Oxypetalum* extract renders the metal surface of sample (c) with evidence of deposition. The deposit is attributed to surface protection [31]. The surface deposition of *E. oxypetalum* supports the adsorption model and the increases inhibition efficiencies recorded at the gravimetric and the EIS techniques.

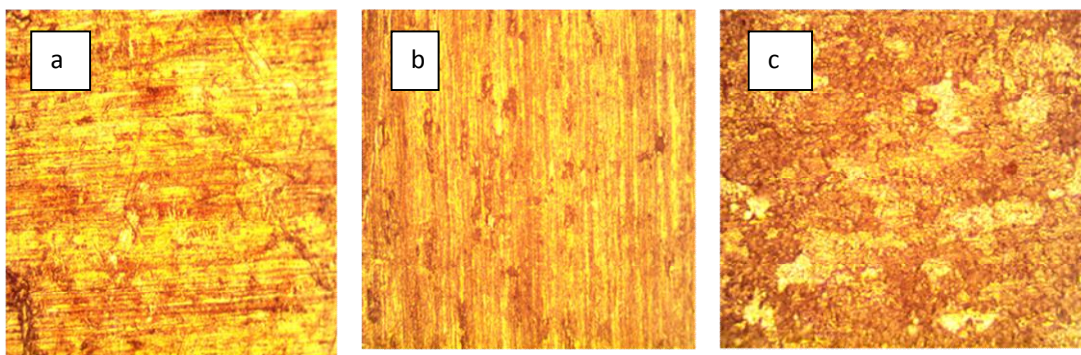


Fig. 10. Optical Micrograph of AA5052 alloy (a) Raw Material, (b) exposed to inhibitor-free (c) exposed to inhibited environment

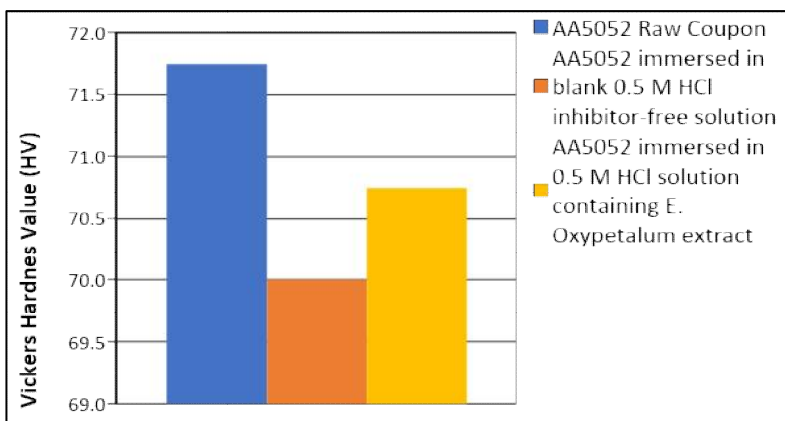


Fig. 11. Mechanical Vickers micro indentation value of AA5052 exposed to 0.5 M HCl solution

3.7 Vickers Micro-indentation Test

Hardness broadly defined as the resistance to permanent surface indentation or penetration by [32] paves the need for microindentation hardness testing (MHT) conducted on AA5052. The mechanical hardness test of AA5052 was investigated using Vickers's indentation technique. A load of 10 kgf (N) was notched on four different random locations on the coupons. The influence of the inhibitor developed was accessed based on the Vickers Pyramid number (HV). The Vickers's number value of the coupon dipped in the inhibitor-free solution is lower compared with that exposed to inhibitor environment; while the value of the raw material is the highest. This implies that the adsorption of *E. oxypetalum* extract rescued the AA5052 alloy from corrosion since corrosion process is involved in material loss and mechanical test is relative to the thickness of the material. It was revealed (Fig. 11) that the presence of *E. oxypetalum* extract. These scale change in the HV confirms another potency of *E. oxypetalum*.

4. CONCLUSION

The influence of eco-friendly leaf extract of *E. oxypetalum* on the corrosion process of aluminum alloy AA5052 has been investigated in 0.5 M HCl environment using gravimetric and electrochemical impedance spectroscopy. The following conclusion have been made based on the introduction of different concentration of *E. oxypetalum* leaf extract in 0.5 M HCl solution:

1. The introduction of *E. oxypetalum* in the corrosive media reduced the weight loss and the corrosion rate of AA5052 alloy.
2. EIS method reveals that the charge-transfer resistance increases with increase in inhibitor concentration.
3. The inhibition efficiency of the green inhibitor increases with increasing inhibitor concentration, but reduced with temperature rise.
4. The E_a increase with inhibition introduction confirms adsorption of the inhibitor molecules on the metal surface as it created double layer.
5. Decrease of the entropy on the addition of the inhibitor extract explains the association interaction of the inhibitor molecules. While the heat of adsorption increase supports the evidence of adsorption on the metal/solution interface.

6. Adsorption isotherm of *E. oxypetalum* on the AA5052 surface follows Langmuir's adsorption isotherm. Adsorption was through physical adsorption.
7. Inhibition process followed first order reaction kinetic. The process was spontaneous according to the Gibb's free energy.
8. The mechanical hardness strength of the ingot was preserved due to adsorption of the inhibitor molecules of the metal surface. And surface rescued the metal surface from attack as revealed by the surface morphology.

ACKNOWLEDGEMENT

The author thanks the Nigerian Government agency, Tertiary Education Trust Fund (TETFund) for the sponsorship in conducting this research.

COMPETING INTERESTS

Author has declared that no competing interests exist.

REFERENCES

1. Karthik G, Sundaravadivelu M. Studies on the inhibition of mild steel corrosion in hydrochloric acid solution by atenolol drug. Egyptian Journal of Petroleum. 2016;25(2): 183-191.
2. Obot IB, Obi-Egbedi NO. Theoretical study of benzimidazole and its derivatives and their potential activity as corrosion inhibitors. Corrosion Science. 2010;52(2): 657-660.
3. Li X, Tang L, Li L, Mu G, Liu G. Synergistic inhibition between o-phenanthroline and chloride ion for steel corrosion in sulphuric acid. Corrosion Science. 2006;48(2):308-321.
4. Palou RM, Olivares-Xomelt O, Likhanova NV. Environmentally friendly corrosion inhibitors, in Developments in corrosion protection; 2014. IntechOpen.
5. Yıldırım A, Cetin M. Synthesis and evaluation of new long alkyl side chain acetamide, isoxazolidine and isoxazoline derivatives as corrosion inhibitors. Corrosion Science. 2008;50(1):155-165.
6. Okafor PC, Zheng Y. Synergistic inhibition behaviour of methylbenzyl quaternary imidazoline derivative and iodide ions on

- mild steel in H₂SO₄ solutions. Corrosion Science. 2009;51(4):850-859.
7. Al-Amiery AA, Ahmed MHO, Abdullah TA, Gaaz TS, Kadhum AaH. Electrochemical studies of novel corrosion inhibitor for mild steel in 1 M hydrochloric acid. Results in Physics. 2018;9:978-981.
 8. Edward G. Corrosion resistance of aluminum and magnesium alloys: Understanding, performance and testing. John Wiley & Sons. 2010;12.
 9. Astm G. G 1-03: Standard practice for preparing, cleaning and evaluating corrosion test specimens. Philadelphia, Pennsylvania: American Society for Testing and Materials; 2003.
 10. Internasional A. ASTM G31-72: Standard practice for laboratory immersion corrosion testing of metals. United State; 2004.
 11. Kelly RG, Scully JR, Shoesmith DW, Buchheit RG. Electrochemical techniques in corrosion science and engineering. Basel, New York: Marcek DEkker, Inc.; 2003.
 12. Lasia A. Electrochemical impedance spectroscopy and its applications. New York: Kluwer Academic/Plenum Publishers. 1999;32.
 13. Astm E. E 384 – 99 Standard test method for microindentation hardness of materials. Annual Book of ASTM Standards. 1999;3.
 14. Callister WD, Rethwisch DG. Materials science and engineering: An introduction. John Wiley and Sons. Inc., London. 2015;9.
 15. Oguzie EE, Iheabunike ZO, Oguzie KL, Okukwe CE, Chidiebere MA, Enenebeaku CK, Akalezi CO. Corrosion inhibiting effect of Aframomum melegueta extracts and adsorption characteristics of the active constituents on mild steel in acidic media. Journal of Dispersion Science and Technology. 2013;34(4):516-527.
 16. Atta AM, El-Mahdy GA, Allohedan HA, Abdullah MM. Adsorption characteristics and corrosion inhibition efficiency of ethoxylated octadecylamine ionic liquid in aqueous acid solution. Int. J. Electrochem. Sci. 2016;11:882-898.
 17. Yadav DK, Quraishi MA. Application of some condensed uracils as corrosion inhibitors for mild steel: Gravimetric, electrochemical, surface morphological, UV-visible and theoretical investigations. Industrial & Engineering Chemistry Research. 2012;51(46):14966-14979.
 18. Awiri GO, Osarolube E. Inhibitive action of *Aloe vera* on the corrosion of copper and brass in different media. Scientia Africana. 2010;9(2):51-58.
 19. Qin TT, Li J, Luo HQ, Li M, Li NB. Corrosion inhibition of copper by 2, 5-dimercapto-1, 3, 4-thiadiazole monolayer in acidic solution. Corrosion Science. 2011;53(3):1072-1078.
 20. Ashassi-Sorkhabi H, Shabani B, Aligholipour B, Seifzadeh D. The effect of some Schiff bases on the corrosion of aluminum in hydrochloric acid solution. Applied Surface Science. 2006;252(12): 4039-4047.
 21. Noor EA. The inhibition of mild steel corrosion in phosphoric acid solutions by some N-heterocyclic compounds in the salt form. Corrosion Science. 2005;47(1):33-55.
 22. James AO, Akaranta O. Corrosion inhibition of aluminum in 2.0 M hydrochloric acid solution by the acetone extract of red onion skin. African Journal of Pure and Applied Chemistry. 2009;3(12): 262-268.
 23. Oguzie EE. Studies on the inhibitive effect of *Occimum viridis* extract on the acid corrosion of mild steel. Materials Chemistry and Physics. 2006;99(2-3):441-446.
 24. Inglezakis VJ, Zorpas AA. Heat of adsorption, adsorption energy and activation energy in adsorption and ion exchange systems. Desalination and Water Treatment. 2012;39(1-3):149-157.
 25. Obot IB, Obi-Egbedi NO, Umoren SA, Ebenso EE. Synergistic and antagonistic effects of anions and *Ipomoea involucreta* as green corrosion inhibitor for aluminium dissolution in acidic medium. International Journal of Electrochemical Science. 2010;5(7):994-1007.
 26. Bhajiwala H, Vashi R. Ethanolamine, diethanolamine and triethanolamine as corrosion inhibitors for zinc in binary acid mixture [HNO₃+ H₃PO₄]. Bulletin of Electrochemistry. 2001;17(10):441-448.
 27. Iroha N, Hamilton-Amachree A. Adsorption and anticorrosion performance of *Ocimum canum* extract on mild steel in sulphuric acid pickling environment. American Journal of Materials Science. 2018;8(2):39-44.
 28. Muthukrishnan P, Jeyaprabha B, Prakash P. Adsorption and corrosion inhibiting behavior of *Lannea coromandelica* leaf

- extract on mild steel corrosion. Arabian Journal of Chemistry. 2017;10:2343-2354.
29. Ebenso EE, Isabirye DA, Eddy NO. Adsorption and quantum chemical studies on the inhibition potentials of some thiosemicarbazides for the corrosion of mild steel in acidic medium. International Journal of Molecular Sciences. 2010;11(6): 2473-2498.
30. Abeng FE, Idim VD, Nna PJ. Kinetics and thermodynamic studies of corrosion inhibition of mild steel using methanolic extract of *Erigeron floribundus* (Kunth) in 2 M HCl solution. World News of Natural Sciences. 2017;10:26-38.
31. Dehghani A, Bahlakeh G, Ramezanzadeh B. A detailed electrochemical/theoretical exploration of the aqueous Chinese gooseberry fruit shell extract as a green and cheap corrosion inhibitor for mild steel in acidic solution. Journal of Molecular Liquid. 2019;282:366–384.
32. Powers JM, Sakaguchi RL, Craig RG, Craig's restorative dental materials/edited by Ronald L. Sakaguchi, John M. Powers. Philadelphia, PA: Elsevier/Mosby; 2012.

© 2020 Nwosu; This is an Open Access article distributed under the terms of the Creative Commons Attribution License (<http://creativecommons.org/licenses/by/4.0>), which permits unrestricted use, distribution, and reproduction in any medium, provided the original work is properly cited.

Peer-review history:

*The peer review history for this paper can be accessed here:
<http://www.sdiarticle4.com/review-history/57465>*